Aspects of Molecular Medicine 5 (2025) 100064

Contents lists available at ScienceDirect

Aspects of Molecular Medicine

journal homepage: www.journals.elsevier.com/aspects-of-molecular-medicine

In vitro and in silico Anti-diabetes mechanism of phytochemicals from *Curculigo pilosa* and its pharmacokinetic profiling via α-amylase inhibition

Damilola A. Omoboyowa [a,*], Temitope C. Aribigbola [a], Simbo T. Akinsulure [a], Damilola S. Bodun [a], Ezekiel A. Olugbogi [b], Ebenezer A. Oni [a]

[a] *Phytomedicine and Computational Biology Lab., Department of Biochemistry, Adekunle Ajasin University, Akungba-Akoko, Ondo State, Nigeria*
[b] *Department of Biochemistry, Babcock University, Ilesan Remo, Ogun State, Nigeria*

ARTICLE INFO

Handling Editor: Prof A Angelo Azzi

Keywords:
Diabetes
Curculigoside
α-amylase
In silico
In vitro

ABSTRACT

Diabetes mellitus is characterized by elevated blood glucose resulting from carbohydrate metabolism via glucose metabolizing enzymes such as α-amylase. *Curculigo pilosa* is traditionally used as herbal medication as anti-diabetes therapy but its mechanism of action is yet to be explored. This study investigates α-amylase inhibitory potential of *C. pilosa* using in vitro and in silico approaches. The ethylacetate, n-butanol and methanol extracts of *C. pilosa* were subjected to in vitro α-amylase inhibitory assay, followed by identification of the bioactive compounds from the most potent extract using HPLC. Integrated computational analyses were performed on ten (10) active compounds against α-amylase using Maestro Schrodinger (v2). The results of the in vitro α–amylase assay revealed n-butanol extract as the potent extract with IC_{50} of 132.70 μg/mL, although the standard drug (acarbose IC_{50} = 128.70 μg/mL) inhibits α-amylase better than the extracts. The HPLC result revealed the presence of ten (10) active compounds. Acarbose was observed to possess better binding affinity (−11.502 kcal/mol) than all the compounds but curculigoside was the hit compound with binding affinity of −8.797 kcal/mol. Some of the compounds showed appreciable inhibitory pIC_{50} and fitness scores comparable to the standard drug. The pharmacokinetic profile revealed that none of the compounds violated more than one Lipinski's rule of five while the standard drug (acarbose) violated three (3) of the rules. The root mean square deviation shows reasonable level of stability within the simulation period for both curculigoside and acarbose. The result of in silico study showed significant inhibitory potential of the active compounds against α-amylase which was consistent with the in vitro inhibition of α amylase by the plant extract suggesting this as the possible mechanism of antidiabetes action of *C. pilosa*.

1. Introduction

Diabetes mellitus is a chronic metabolic disorder of carbohydrates, protein, and lipids which result in elevated blood sugar levels. Some of the most prevalent symptoms of diabetes mellitus include polyuria, polyphagia, polydipsia, fatigue, weight loss, and prolonged wound healing (Balaji et al., 2019). Pathological characteristics of diabetes mellitus include elevated blood glucose levels which arise either from lack of insulin as in type one, or from the inability of the body to effectively use insulin. When insulin is not correctly used, it prevents the proper absorption of glucose by various cells causing chronic hyperglycemia and damage to several tissues and organs. Diabetes mellitus can lead to various life-threatening problems including nephropathy, retinopathy, neuropathy, and other fatal complications (Kawahito and Kitahata, 2009). According to reports from 2017, 424.9 million people worldwide developed diabetes mellitus (DM), which corresponds to nearly 8.8% of the adult population. The World Health Organization (WHO) had previously estimated this figure to be higher in 2014 (Cho et al., 2018). In 2010, 12,81,300 deaths were directly attributable to diabetes mellitus, a 92.7% increase over the 6,65,000 fatalities in 1990 when diabetes was the fifteenth leading cause of death in the world before rising to ninth place in 2010 (Bhutani and Bhutani, 2014).

Currently, available treatments offer good control of major symptoms but do not increase the production of insulin or effective utilization of it, making it essential for novel drug discoveries. Three primary sulfonylurea medications are commonly prescribed, this includes glimepiride, glipizide, and glyburide (Korytkowski, 2004). Nevertheless, these medications have limited effectiveness with many associated side

* Corresponding author.
E-mail address: damilola.omoboyowa@aaua.edu.ng (D.A. Omoboyowa).

https://doi.org/10.1016/j.amolm.2025.100064
Received 20 November 2024; Received in revised form 29 December 2024; Accepted 27 January 2025
Available online 31 January 2025
2949-6888/© 2025 The Authors. Published by Elsevier B.V. This is an open access article under the CC BY-NC license (http://creativecommons.org/licenses/by-nc/4.0/).

effects. The availability of pre-clinical and clinical trials on mild to moderate diabetes mellitus is timely for developing more effective and safe natural alternatives. While synthetic agents have had limited success in serving as potential drugs for managing diabetes mellitus, challenges in terms of pharmacokinetics and safety factors continue to pose significant hurdles (Aathira and Jain, 2014). Natural products, on the other hand, provide effective and safe pharmacodynamic attributes in cases of complex metabolic conditions. However, the unavoidable obstacles in the path of developing drugs for diabetes mellitus persist due to the numerous biological pathways and metabolism as a result of the disease, the damaging of certain organs including the pancreas, kidney, and liver, and other complications as a result of the condition.

In the digestive system, α-amylase breaks down internal α-1, 4-glycosidic bonds of starch into glucose and maltose. Pancreatic amylase is produced in the small intestine by the pancreas, whereas salivary amylase is located in salivary glands (Woolnough et al., 2008). By accelerating the digestion of starch and disaccharides, α-amylase can regulate blood glucose levels. Inhibiting carbohydrate hydrolyzing enzymes like α-amylase and glucosidases slows down the absorption of glucose; this is one of the therapeutic methods for reducing the rise in blood sugar levels after a meal (Nair et al., 2013). Since only monosaccharides can be absorbed and delivered into the bloodstream, the complex components of carbohydrates in diets are broken down into monosaccharides by the enzymes. The inhibition of these enzymes is thought to be a key strategy in the management of postprandial blood glucose levels linked to type-2 diabetes because it can significantly increase the overall time of carbohydrate digestion and reduce the increase in blood glucose level after a carbohydrate diet intake (Kim et al., 2011).

Plant-derived natural products as well as their bioactive compounds have been widely researched in recent years for their therapeutic potential in a range of metabolic diseases including diabetes mellitus. Numerous extracts of traditional plants have been reported to have an excellent anti-diabetic effect based on the findings of several works of metabolic research. The *Curculigo pilosa* (African crocus) rhizome was the first African species of Curculigo to be reported (Wang et al., 2021). It is frequently used as a laxative as well as for the treatment and management of diabetes (Karigidi and Olaiya, 2021). As alternative medicine, *C. pilosa* is used in the treatment of sexually transmitted infections and heart disease (Nie et al., 2013). The extract of the plant rhizome has been reported to be rich in polyphenols and possess antioxidant, antimicrobial, erectogenic and hypoglycemic potentials (Karigidi et al., 2019; Adefegha et al., 2016; Gbadamosi and Egunyomi, 2010). Although the anti-diabetes potential of *C. pilosa* has been reported, the mechanism of anti-diabetes action of the phytochemicals present in the plant has not been explored, hence, this study investigates α-amylase inhibitory potential of the phytochemicals identified from butanol extract of *C. pilosa* rhizome.

2. Materials and methods

2.1. Procurement of C. pilosa rhizomes

The *C. pilosa* rhizomes used for this study were purchased from Okitipupa main market, Southwest Nigeria. The plant was identified and authenticated by a botanist at the Department of plant science and Biotechnology, Adekunle Ajasin University, Akungba-Akoko, Nigeria with the voucher number (PSBH-2308) deposited.

2.2. Extraction of C. pilosa rhizome

Fresh *C. pilosa* rhizomes were rinsed with water, cut into pieces, air-dried at room temperature for three weeks, and milled using a mechanical blender. Exactly 176 g of the powdered rhizome was macerated with 1 L (1000 mL) of ethylacetate for 72 h. Thereafter, the solvent-plant mixture was filtered, and the filtrate was allowed to pass through Whatman No 1 filter paper, then concentrated with a rotary evaporator and allowed to dry as ethylacetate extract (EE). The residue was soaked in 1000 mL of n-butanol, and separated after 72 h; the filtrate was filtered, concentrated, and dried as n-butanol extract (BE). The residue was further soaked in 1000 mL of methanol, separated after 72 h, filtered with filter paper, concentrated, and dried as methanol extract (ME). The three extracts (EE, BE, ME) were subjected to in vitro antioxidant assays. Ethylacetate and butanol were considered for extraction because the plant is reportedly rich in polyphenols while methanol was used to extract the remaining highly non-polar compounds from the residues.

2.3. In vitro α-amylase inhibition assays

α-Amylase inhibitory potential of the extracts was estimated by the method of Worthington (1993) as reported by Omoboyowa et al. (2024). Exactly 500 µl of the extracts (500–2000 µg/mL) and 500 µl of buffer (0.02 M sodium phosphate with 0.006 M NaCl, pH 6.9) containing α-amylase (0.5 mg/mL) were incubated at room temperature (25 °C) for 10 min. After which, 500 µl of starch solution (1%) prepared with phosphate buffer (0.02 M) was added. The control was prepared without the sample. The solution was kept for 10 min at 25 °C. The reaction was stopped by introducing dinitrosalicylic acid (DNSA), the absorbance was taken spectrophotometrically at 540 nm against balnk after incubating at 100 °C for 5 min and allowed to cool.

$$Inhibition\ percentage = \frac{Abs\ of\ control - Abs\ of\ sample}{Abs\ of\ control} \times 100$$

2.4. High-performance liquid chromatography (HPLC) analysis of C. pilosa

Based on the in vitro α-amylase inhibitory result, the n-butanol extract (BE) was observed to be the most potent; it was therefore subjected to HPLC analysis according to the method reported by Omoboyowa et al. (2023a). Briefly, 5 g of the extract was dissolved in 20 mL of acetonitrile/methanol at ratio 10:1 and mixed vigorously for 30 min. The organic solvent was separated into a 25 mL flask and made up to the mark. The HPLC machine (Shi-Madzu Co., Kyoto, Japan; with a fluorescence detector (RF- 10AXL), Prominence pump (LC-20AD; Shimadzu), Hypersil GOLD column (4.6 × 250 cm, 5 µm and column oven (CTO-10ASvp; Shimadzu)) was associated with a mass detector to form liquid chromatography-mass spectrometry (LC-MS). The extract was filtered using the syringe filter and 50 µl of the filtrate was inserted into the HPLC at a flow rate of 1 mL/min and running time of 50 min to generate the corresponding peak profile of the extract in the chromatograph. The key validation parameters for the HPLC protocol include: accuracy, precision, specificity and linearity by evaluating factors like peak shape, retention time, and response to varying concentrations. The separated substances were transferred to the mass spectrometer, ionizing the compounds and their fractions in the mass spectrometer through mass analyzer to identify the ions based on their mass-to-charge rations.

3. In silico analysis

3.1. Preparation of compounds

The library of ten (10) compounds identified from butanol extract of *C. pilosa* rhizome via HPLC and the standard drug (acarbose) were selected for this study, 3D (.SDF) format of the selected library of compounds was retrieved from the NCBI PubChem database (www.ncbi.nlm.nih.gov). The LigPrep interface of the 2017-V2 version of Schrödinger was used to prepare the retrieved ligands at the force field of OPLS3 and pH 7 (±2) using Epik. Desalt and generate tautomers were also selected on the LigPrep interface and the stereoisomer computation

was left to retain specific chiralities (vary other chiral centers) and to generate at most 1 per ligand.

3.2. Target protein preparation and docking procedure

The crystallographic structure of human pancreatic α-amylase (PDB ID = 2QV4) was retrieved from www.rcsb.org, the monomeric (chain A) protein was prepared using the protein preparation wizard of Schrodinger suit (2017 v2). The receptor grid generation tool of the software was used to generate a grid coordinate (x = 36.71, y = 45.14, and z = 52.40) at the binding domain of the co-crystalized ligand (Omoboyowa, 2024).

The prepared compounds were virtually screened against the target's binding site where the grid coordinate has been generated based on the co-crystalized ligand. To estimate the binding affinity, extra precision flitering procedure was used to perform the site directed docking of the bioactive compounds and the control drug (acarbose) and the 2D interaction of the protein-ligand complexes was visualized with Discovery Studio 2020.

3.3. Fitness score estimation via pharmacophore modeling

The receptor-ligand complex of the pharmacophore hypothesis of maestro suit (2017-v2) was involved in modeling the hypothesis for the α-amylase-co-crystalized ligand complex. The hypothesis obtained was used to analyze the bioactive compounds from *C. pilosa* extract after preparation of the compounds. The screening of the compounds was performed using the phase screen module of the pharmacophore hypothesis and their fitness scores were evaluated (Omoboyowa, 2022).

3.4. PIC_{50} estimation via QSAR model

The recovery of the dataset containing the α-amylase experimental inhibitors with their respective PIC_{50} from the CHEMBL (https://www.ebi.ac.uk/chembl/) database was performed using the FASTA sequence of α-amylase. Data-warrior was used to convert the dataset to ".sdf" format. The saved sdf file was imported to the workspace of Maestro software for preparation using the macro model minimization tool, and the PIC_{50} of the molecules was used to develop the QSAR model of the protein (Omoboyowa, 2022). The PIC_{50} of the bioactive compounds from *C. pilosa* rhizome were evaluated based on the best model.

3.5. Screening for ADME profile

The pharmacokinetic and drug-likeness profile of the bioactive compounds from *C. pilosa* was predicted by the Qikprop tool of Schrodinger suite (2017-v2).

3.6. Molecular dynamics simulation

The molecular dynamics (MD) simulation of the top compound (Curculigoside) and Acarbose were performed using the Desmond. Curculigoside was selected as the hit compound based on the binding affinity, pharmacokinetics profile, PIC50 and fitness scores. The complexes were simulated in an explicit solvent system at $300^{O}K$ and 1.01325 bar with Na^{+}, and Cl^{-} added to maintain neutrality. With all parameters at default, the MD simulation was performed with transferable intermolecular potential-4 point (TIP4P) force field. The MD trajectories were evaluated for root mean square deviation (RMSD), root mean square fluctuation (RMSF), radius of gyration, and protein-ligand contacts (Omoboyowa et al., 2023b).

3.7. Statistical analysis

The statistical analyses of the data obtained were carried out by GraphPad Prism 9, one way analysis of variance was used for the data analyses, followed by Dunnett's post hoc test. $P < 0.05$ was considered statistically significant. Results are presented as mean and SEM.

4. Results

4.1. In vitro α-amylase inhibition

The result of the α-amylase inhibitory potential of *C. pilosa* solvent extracts presented in Fig. 1a revealed that all the extracts across the concentrations showed significant ($P < 0.05$) reduction in percentage α-amylase inhibition compared with the standard drug (acarbose). The n-butanol extract was observed to show a higher percentage α-amylase inhibition across the concentration than other solvent extracts of the plant. Hence the selection of n-butanol extract for high-performance liquid chromatography to identify the active compounds. Fig. 1b presented the percentage normalized response against the logarithm of α-amylase concentration that was used to estimate the IC_{50} of the extracts. As shown in Table 1, the standard drug (acarbose) showed the lowest IC_{50} of 128.70 μg/mL compared with the extracts. Among the extracts, n-butanol showed the lowest IC_{50} of 132.70 μg/mL followed by the methanol extract with IC_{50} of 180.20 μg/mL.

4.2. Identification of bioactive compounds in BECP using HPLC

The bioactive compounds present in butanol extract of *C. pilosa* (BE) were identified using HPLC; ten (10) peaks depicting 10 active compounds were observed in the HPLC chromatogram. The compounds were observed to include sitosterol, curculigol, curculin, curculigenin A, curculigenin B, curculigoside, stigmasterol, phlorizin, pomiferin and scandenin. From Supplementary Figs. 1 and 2 and Table 2, curculigol showed the highest peak and composition of 24.42 ppm, while scandenin showed the lowest peak among the bioactive compounds. The structure of the bioactive compounds is presented in Fig. 2.

4.3. Results of molecular docking study

Using molecular docking, the binding affinities of HPLC-identified compounds were compared to acarbose (reference drug). The results showed that none of the HPLC-identified compounds exhibited better binding affinity than acarbose, with their docking scores ranging from −8.797 to −4.446 kcal/mol as shown in Fig. 3.

Pomiferin, with a docking score of −5.552 kcal/mol, formed three hydrogen bonds with GLN 63, GLU 233, and ARG 195, along with a Pi-anion bond with ASP 300. Phlorizin achieved a high docking score of −7.099 kcal/mol, forming five hydrogen bonds with ASP 300, ARG 195, GLN 63, and THR 163, and two special Pi-Pi stacked bonds with TYR 62 and TRP 59. Acarbose the reference drug, with the highest docking score of −11.502 kcal/mol, formed eight hydrogen bonds with HIS 305, GLU 233, HIS 201, LYS 200, GLU 240, GLN 63, TRP 59, and HIS 101, along with a Pi-alkyl bond with ILE 235. Curculigoside, the top-ranked compound among the HPLC-identified compounds, achieved a docking score of −8.797 kcal/mol, forming three hydrogen bonds with GLU 233, ASP 300, and GLN 63. Stigmasterol formed a single hydrogen bond with ASP 300, while scandenin formed two hydrogen bonds with GLN 63 and ASP 197, and two Pi-Pi stacked bonds with TRP 59 and TYR 62. Curculigol formed two hydrogen bonds with ARG 195 and ASP 300 (Fig. 4).

4.4. Pharmacophore modeling and phase screening of the bioactive compounds

In this study, to understand how the co-crystallized ligand interacts with the α-amylase, we used an E-pharmacophore model to identify steric properties of the co-crystallized ligand that were critical for optimal interaction with the target protein. The model was then applied to screen the HPLC-identified phytochemicals, allowing us to view if these HPLC compounds have the same steric features present in the co-

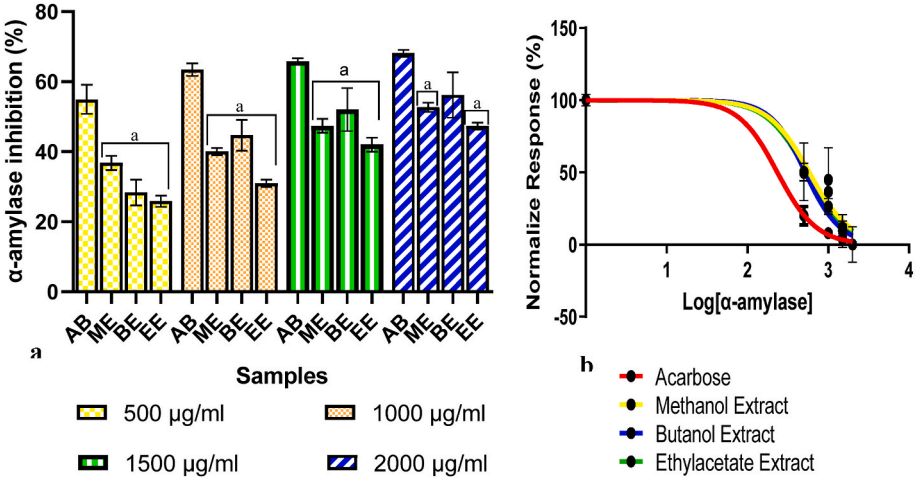

Fig. 1. (a) Percentage α-amylase inhibition (b) Normalize response curve of various extracts of *Curculigo pilosa* rhizome
AB: Acarbose; ME: methanol Extract; BE: *n*-butanol Extract; EE: Ethylacetate Extract.

Table 1
IC_{50} of solvent extracts of *C. pilosa* rhizome.

Parameters	Acarbose	Methanol Extract	Butanol Extract	Ethylacetate Extract
Log IC_{50}	2.11	2.58	2.52	2.64
IC_{50} (µg/ml)	128.70 ± 0.21	180.20 ± 1.43	132.70 ± 2.15	234.30 ± 2.98
R^2	0.9829	0.9122	0.9888	0.9463

Table 2
Bioactive compounds from n-butanol extract of *Curculigo pilosa*.

S/N	Compounds	Retention time	Area	Composition (ppm)
1	Sitosterol	1.16	33.16	3.322
2	Curculigol	1.30	244.10	24.410
3	Curculin	1.85	102.78	10.283
4	Curculigenin A	2.18	73.19	7.322
5	Curculigenin B	3.05	73.00	7.303
6	Curculigoside	4.00	84.10	8.411
7	Stigmasterol	5.32	74.50	0.002
8	Phlorizin	6.20	391.25	0.001
9	Pomiferin	8.47	34.99	0.003
10	Scandenin	9.48	37.43	0.002

crystallized ligand. By comparing the features of these compounds to those of the co-crystallized ligand and evaluating their similarity, we were able to determine their fitness scores. The hypothesis model for the optimal interaction of the co-crystallized ligand with α-amylase consists of seven (7) features which include five hydrogen bond donors and two hydrogen acceptors as shown in Fig. 5. The fitness score of the HPLC-identified compounds is shown in Table 3. The higher the fitness score, the higher the predicted biological activity of that compound to the target. Curculin, had the highest fitness score, 1.256, more than the co-crystallized ligand itself, acarbose with a fitness score of 1.056. Also, Curulingoside (the top compound by docking score) and Curculigenin A had better fitness scores than acarbose with 1.156 and 1.133 as fitness scores respectively.

4.5. PIC_{50} prediction of bioactive compounds via QSAR modeling

The biological activity of chemical compounds are predicted based on their molecular structure using the Quantitative structure-activity relationship (QSAR) modeling. Other machine learning models including support vector machines, neural networks and decision trees may be employ to train the models generated from the compounds' chemical described dataset. Herein, AutoQsar modeling of the target inhibitors automatically divides datasets into 25% test and 75% train sets. The best model by ranking is selected and used to predict the bioactivity of the HPLC-identified compounds. The test and train data sets of the observed and expected activity of the model was depicted in the scatter plot presented in Fig. 6. Based on the predicted bioactivity (PIC_{50}) values, acarbose was predicted to be more active than the HPLC-identified compounds. Curculigenin A was predicted to have the best PIC_{50} value with a score of 5.198 µM. The top compound by docking score, Curculigoside, has predicted bioactivity value of 4.942 µM (Table 4).

4.6. Pharmacokinetic profile of the active comppunds

QPlogHERG measures a molecule's ability to block human ether-a-go-go-related gene (hERG) K^+ channels. Predicted values below −5 suggest significant inhibition, potentially leading to cardiac side effects like sudden cardiac death and QT prolongation. Among the compounds, all except Curculigenin A, Curculigenin B, Curculigol, Sitosterol, and Stigmasterol had values below −5. QPPCaco predicts the permeability of Caco-2 cells. Values above 500 nm/s are considered good, while those below 25 nm/s are poor. Except for acarbose and Phlorizin, all the compounds had predicted values lower than 25. QPlogBB predicts a molecule's ability to pass through the blood-brain barrier. The acceptable range is −3 to 1.2. Only acarbose and Phlorizin did not fall within this range among the compounds as shown in Table 5. None of the HPLC-identified compounds violated more than one of Lipinski's rule of five which indicates their drug likeness but acarbose violated three (3) of these rules.

5. Results of MD simulation

5.1. Root mean square deviation

The root-mean-square deviation (RMSD) measures the average distance of the simulated protein-ligand complex. In the case of α-amylase complexed with acarbose (the standard) as presented in Fig. 7, the Ca atoms showed mean deviations of less than 2.0 Å during the 100 ns simulation which represents stability in the active site. Also, the α-amylase complex with Curculigoside exhibited a stable RMSD value ranging from 4.8 to 6.4 Å from 10 ns to the end of the simulation after a major fluctuation above 4.0 Å. RMSD analysis of protein-fitted ligands assesses how stable the ligands remain within the protein's binding pocket. This suggests that these compounds remain bound to α-amylase without significant diffusion away from the protein.

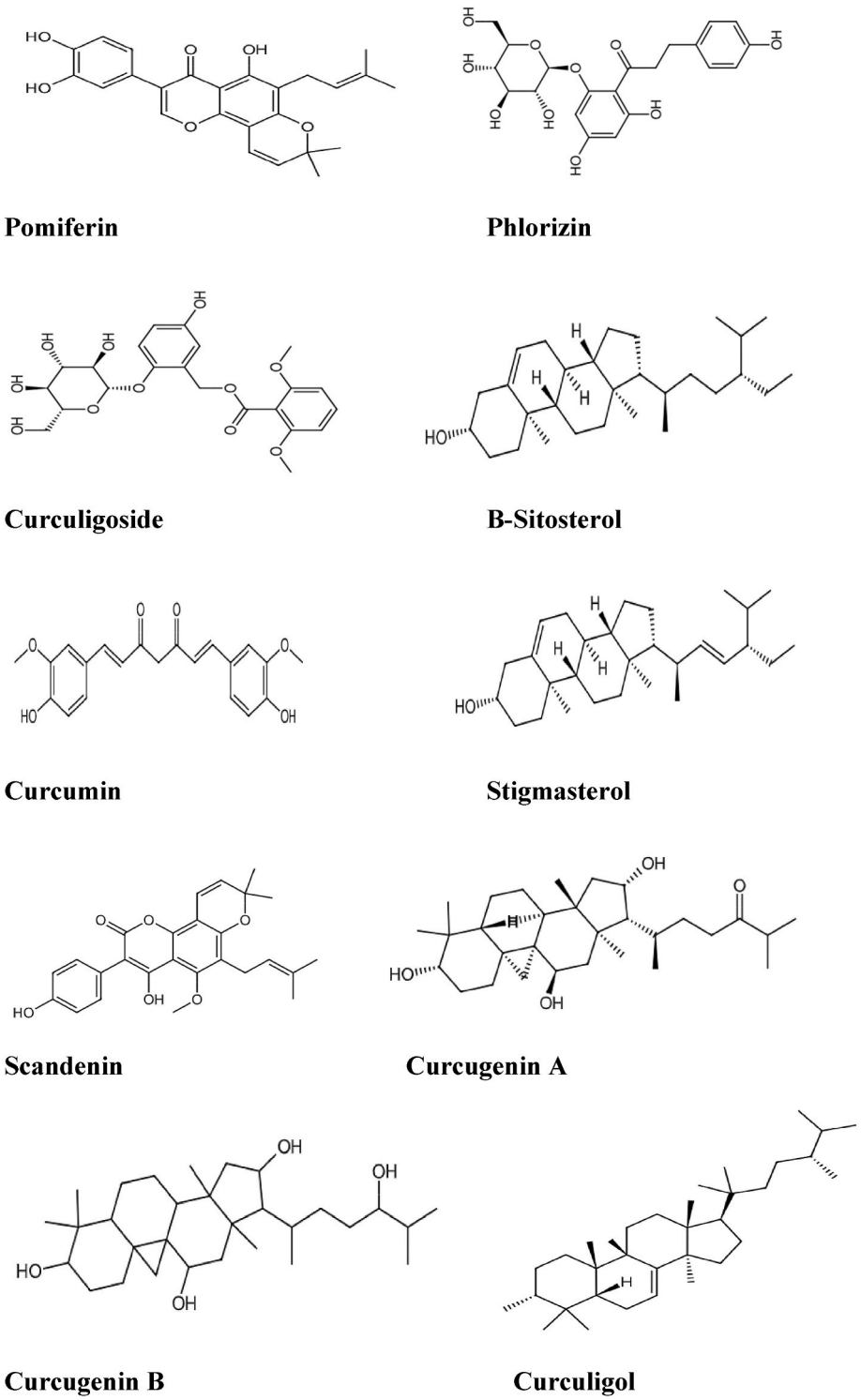

Fig. 2. Structures of Bioactive compounds from HPLC analysis of Butanol extract of *C. pilosa*.

5.2. Root mean sqare flunctuation

The local changes and flexibility of the α-amylase and the compounds in respective complexes were evaluated for root mean square fluctuations (RMSF) analysis throughout the 100 ns simulation trajectories as presented in Fig. 8. RMSF was done to study the flexibility of protein-ligand complexes and fluctuation in interactive amino acid residues in the secondary structure of the target protein. The RMSF plot characterizes the local fluctuations of the residues of the protein. The peaks indicate the residues of the protein that fluctuate the most. Based on the resulting output, the amino acid residues of the α-amylase of the docked complexes had different fluctuations between the amino acid residues during the simulation process of 100 ns. The maximum fluctuation of over 4.0 Å was observed in the Curculigoside – α-amylase complex within the residue 340–360. Overall, the results confirm the better stability of the Acarbose- α-amylase complex compared to the Curculigoside complex due to the fewer fluctuations that occur.

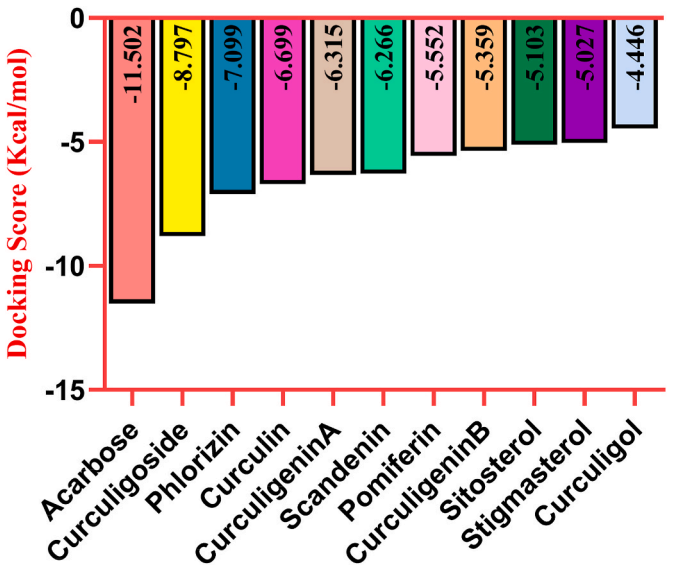

Fig. 3. Graphical representation of the binding affinity.

5.3. *Interaction mapping*

Acarbose formed hydrogen bonds, ionic interactions, water bridges, and hydrophobic contacts with several amino acids, including LYS 278, TRP 280, GLU 282, GLY 283, HIS 331, PRO 332, ARG 398, VAL 401, ASP 402, GLY 403, GLN 404, and ARG 421. However, during molecular docking, it only formed hydrogen bonds with HIS 305, GLU 233, HIS 201, LYS 200, GLU 240, GLN 63, TRP 59, and HIS 101. It exhibited over 200% interaction with ARG 421 during the simulation, an amino acid it didn't interact with during molecular docking.

During the 100ns simulation, Curculigoside formed hydrogen bond interactions with ARG 198, ASP 197, ALA 198, HIS 201, ASP 303, and HIS 305 as shown in Fig. 9. However, most of these interactions lasted less than 20% of the simulation time, except for the interaction with ASP 197. Interestingly, it did not interact with ASP 197 during molecular docking.

6. Discussion

Medicinal plants have provided alternative therapeutic approach to the existing medications for the management of diabetes and its associated complications. *Curculigo pilosa* has been reported for its anti-diabetes activity in ethnomedicinal studies (Nair et al., 2013; Chike-Ekwughe et al., 2023). However, the inhibitory efficacy of this plant against α-amylase has not been explored since one of the therapeutic approaches for diabetes treatment is postprandial glucose reduction by decreasing the rate of glucose absorption which can be achieved through inhibition of the carbohydrate metabolizing enzymes such as α-amylase (Tan et al., 2019). In this study, the in vitro and in silico α-amylase inhibitory activity of *C. pilosa* was investigated to ascertain the probable mechanism of anti-diabetes action. The consideration of α-amylase inhibitory activity alone in this study provide limitation since α-glucosidase is another carbohydrate metabolizing enzyme which would be consider in further study.

The result of the in vitro α-amylase inhibitory study presented in Fig. 1 revealed that, n-butanol extract of *C. pilosa* demonstrated the highest inhibitory potential among the test samples at 1000 µg/mL to 2000 µg/mL followed by the IC_{50} of 132.70 µg/mL. Although the standard drug (acarbose) used in this study showed significant inhibitory α-amylase activity than the extracts presenting IC_{50} of 128.70 µg/mL as shown in Table 1. This result is consistent with the findings of Chike-Ekwughe et al. (2023) who reported that acarbose significantly inhibits α-amylase activity than *Tapinathus cordifolius* leaf solvent fractions. The higher activity demonstrated by the n-butanol extract could be attributed to the presence of bioactive compounds in the extract as shown by the HPLC analysis. From Supplementary Fig. 1 and Table 2, the n-butanol extract was observed to contain vital phytochemicals such as curculigol, curculigenin A, curculigenin B, curculigoside, phlorizin, pomiferin, scandenin (structures shown in Fig. 2), many of these compounds have been linked to the therapeutic activity of medicinal plants for example, Tan et al. (2019) has reported that curculigoside exerts significant anti-diabetes effects in vivo and in vitro by regulating JAK/STAT/NF-Kβ signaling pathway. The anti-diabetes activity of curculigoside derivatives has been reported by Nursamsiar et al. (2022). This compound might contribute to the anti-diabetes property of n-butanol extract of *C. pilosa*. Yet, the molecular docking and simulation results in this study further revealed the α-amylase inhibitory potential of curculigoside as the best among other bioactive compounds from the extract.

Molecular docking is vital in the design and discovery of novel therapeutic agents. It predicts the binding interaction of small molecules and target proteins (Omoboyowa et al., 2023a). According to the results of the molecular docking analysis presented in Fig. 3, all the studied compounds from n-butanol extract of *C. pilosa* showed reduced binding affinity compared with the standard drug (acarbose) with binding affinity of −11.502 kcal/mol. Among the studied compounds, curculigoside showed the highest binding affinity of −8.777 kcal/mol followed by phlorizin (−7.099 kcal/mol). Curculigol was observed to have the lowest binding affinity of −4.446 kcal/mol. This binding affinity can be linked to the interaction of the compounds with the amino acid residues at the binding site of α-amylase. As shown in Fig. 4, acarbose formed eight (8) hydrogen bond with different amino acids while curculigoside formed three (3) hydrogen bond with GLU 233, ASP 300 and GLN 63. The formation of hydrogen bond within small molecule-protein interaction play a pivotal role in establishing the stability of the three dimensional structure of the complex (Pace et al., 2014). Curculigoside with the best binding affinity among the compounds remains promising compared with acarbose despite have lower binding affinity because of the predicted side effects associated with arcabose as it violated three Lipinski's rules as shown in Table 5.

Pharmacophore modeling remain an integral tool in drug discovery. For the identification of vital features in small molecule inhibitory activity (Miller and Roitberg, 2013). Herein, the e-pharmacophore model for α-amylase complexed with acarbose was generated using four hypothesis models. The generated model was presented in Fig. 5. The features used for developing this model includes one H-bond acceptor, hydrophobic interaction, two H-bond donors and one aromatic ring. The screening of the bioactive compounds from n-butanol extract of *C. pilosa* was performed according to these features. According the fitness score result presented in Table 3, curculin, curculigenin A, curculigoside and phlorizin have fitness score higher than 1.00 which is comparable to the standard drug (acarbose). Fitness score is the measure of the rate at which the compounds fit into the binding core of the target with reference to the ligand interaction energies (Natarajan et al., 2015). Hence, curcilin, circuligenin A and curculigoside might be predicted to fit well in the binding site of α-amylase than acarbose. However, all the bioactive compounds reveals positive fitness score showing that they all fit into the protein core.

Quantitative structure-activity relationship (QSAR) is a computational model that showed the relationship between the biological activity of small molecules and their structure (Kwon et al., 2019). This is a vital approach in drug discovery. In this study, the selected model for screening the compounds' PIC_{50} is kpls_desc_47 with 25% test and 75% train set as shown in Fig. 6. The predicted PIC_{50} presented in Table 4 showed that all the bioactive compounds and acarbose have high PIC_{50} above 4.00 µM with acarbose having 6.108 µM as the hieghest, followed by curculigenin A with 5.198 µM. The PIC50 represent negative logarithm of the IC_{50} and is use to compare the efficacy of bioactive

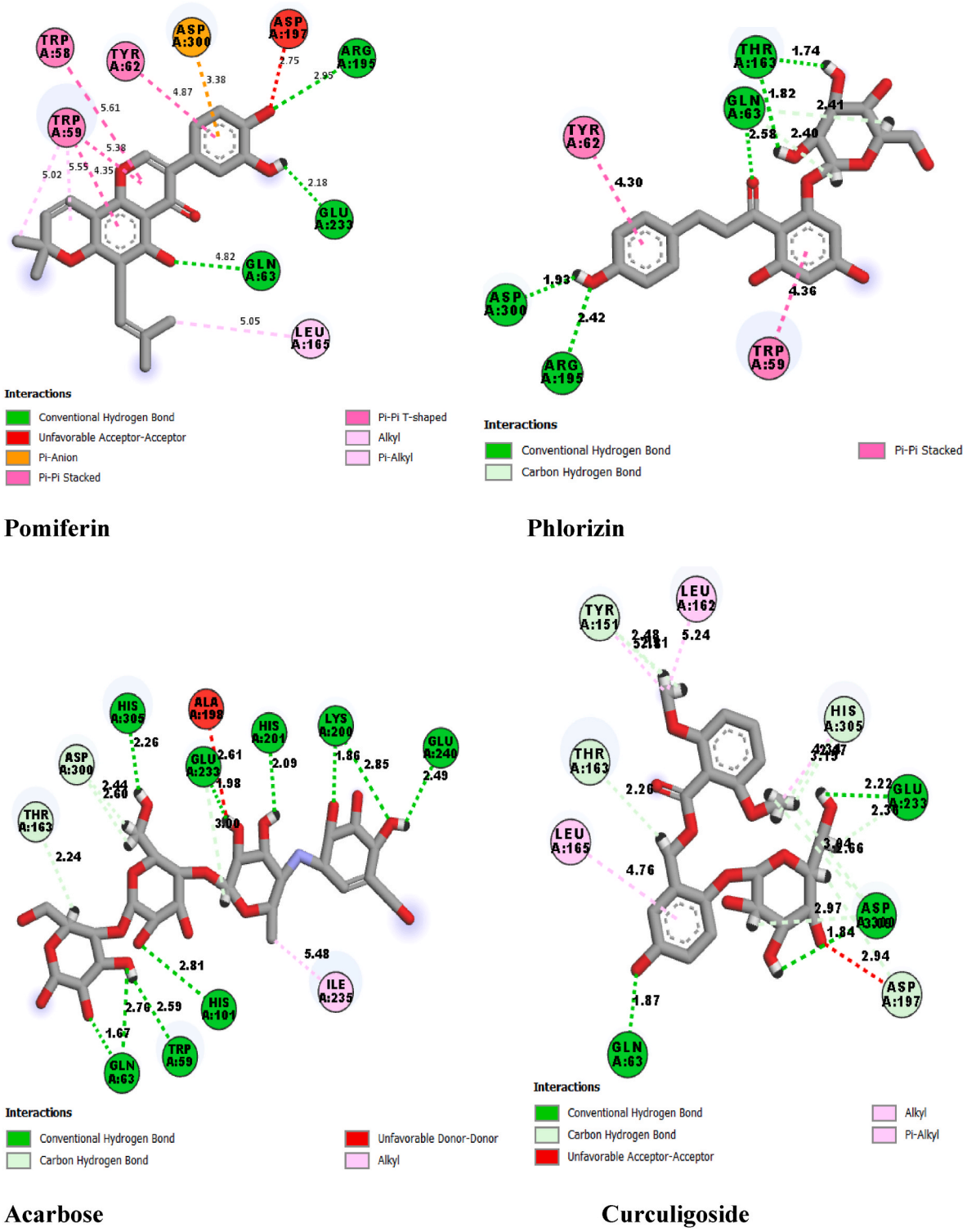

Fig. 4. 2D interaction of bioactive compounds against α-amylase.

compounds at the same molar level with high PIC_{50} denotes exponentially potent inhibitors. This indicate that all the compounds are potent inhibitors of α-amylase.

Although the bioactive compounds from n-butanol extract of *C. pilosa* showed α-amylase inhibitory potential, their pharmacokinetic profiles are critical factor in evaluating their pharmacological efficacy against the target. Novel therapeutic candidates are screened for drug-likeness properties using the Lipinski's rule of five, which takes into account the compounds' molecular weights, hydrogen bond donors and acceptors and lipophilicity (Lipinski et al., 1997). From Table 5, all the bioactive compounds showed molecular weight less than 500 g/mol and obeyed Lipinski's rule of five with maximum of 1 violation of the rule but acarbose was observed to violate three Lipinski rule with high molecular weight of 645.611 g/mol.

Molecular dynamics (MD) simulation is the analysis of the physical movements of atoms and molecules to determine the response of

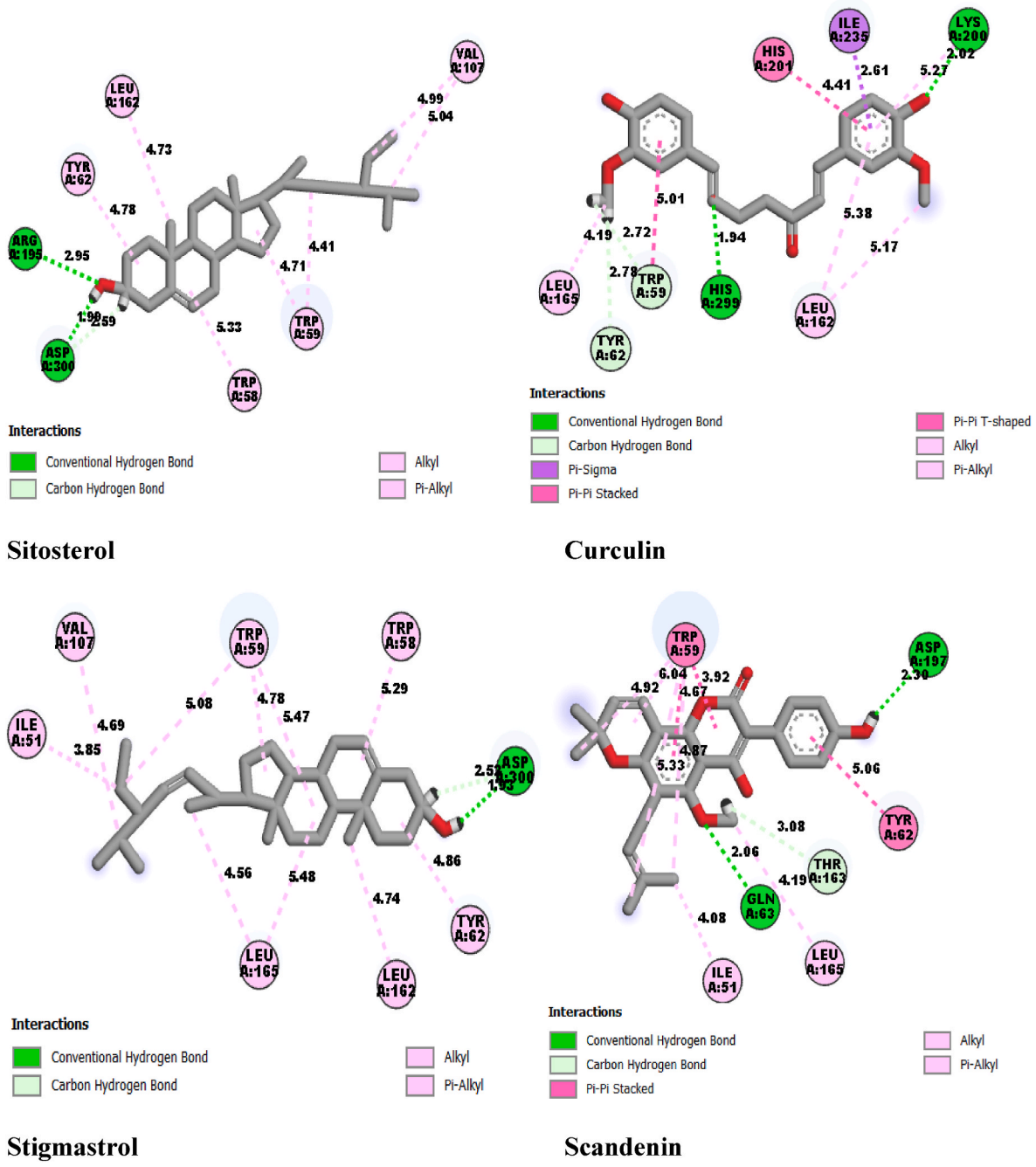

Fig. 4. (*continued*).

biomolecular system to some perturbation (Hollingsworth and Dror, 2018). MD simulation combined with binding free energy calculations are strategy to enhance the factor of virtual screening since it can enrich the accuracy of binding stability prediction of ligand-protein complexes (Liu et al., 2017). In this study, after the evaluation of the post-docking results of the hits, the curculigoside-α-amylase and acarbose-α-amylase complexes were subjected to MD simulation. The root mean square deviation (RMSD), root mean square flunctuation (RMSF) and interaction mapping were analysed from the MD trajectory for 100 ns.

The mobility of the loop and backbone structure of proteins can be predicted from the RMSD analysis. As shown in Fig. 7, both complexes showed slight functuation in the protein structure but there was no significant deviation between the ligand fit on the protein throughout the 100 ns simulation period. This predicted that both curculigoside and acarbose are stable at the core of the target with minimal deviation. The RMSF was used to predict the flunctuation of atoms in the amino acid of α-amlyase during the 100 ns simulation period. RMSF can be used to predict the part of the target that flunctuate most by measuring the deviation of atom from its mean structure over time (Barnett et al., 2018). As shown in Fig. 8, the local changes in the amino acid residues of α-amylase were monitored by calculating the RMSF values of the residues' backbone. The acarbose-α-amylase complex had a maximum flunctuation of 2.4 Å at residue index of 400 while curculigoside - α-amylase complex had flnctuation of above 4.0 Å at 300 residue index. In both complexes, the α-helices and β-strands were observed to be more stable than the unstructured part of the protein. Hence, less flunctuation

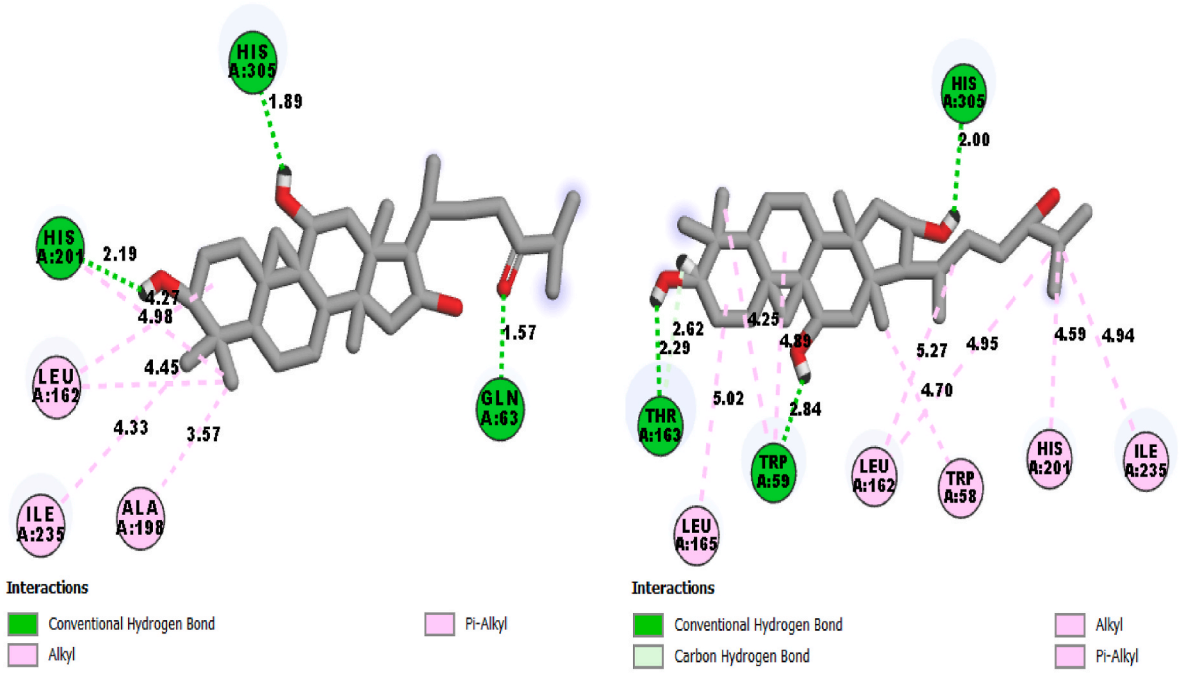

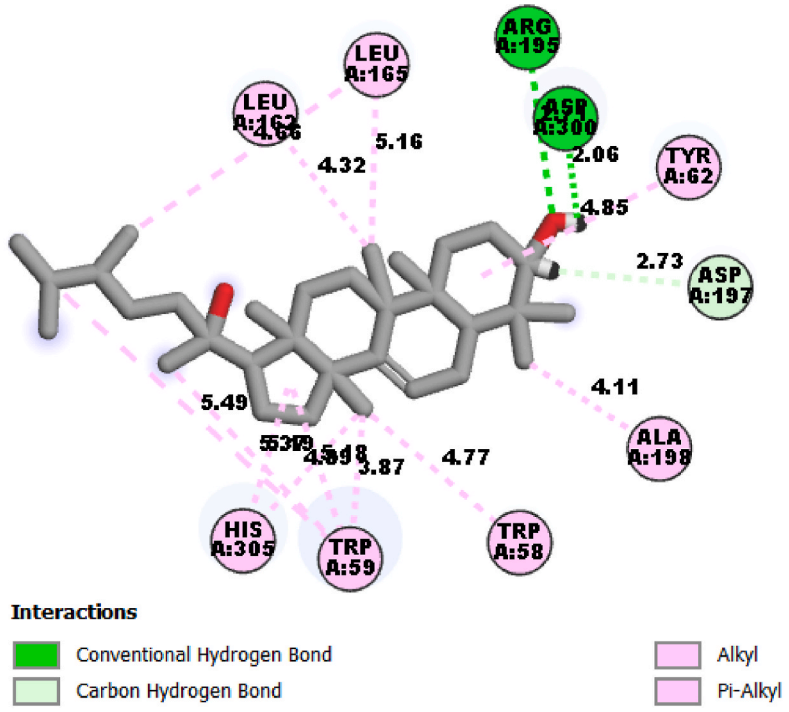

Fig. 4. (*continued*).

was observed. Fig. 9 showed the interaction mapping of the complexes. This interaction analysis is used to study the biological regulation and theoretical basis of drug discovery (Fu et al., 2018). The molecular interaction observed between the compounds and the amino acid residues includes hydrogen bond (H-bond), hydrophobic, water bridges and ionic bond. Acarbose was observed to exhibits high H-bond interaction with vital amino acid residues with ARG 421 showing 2.5 intraction fraction of H-bond. This corroborates the high number of

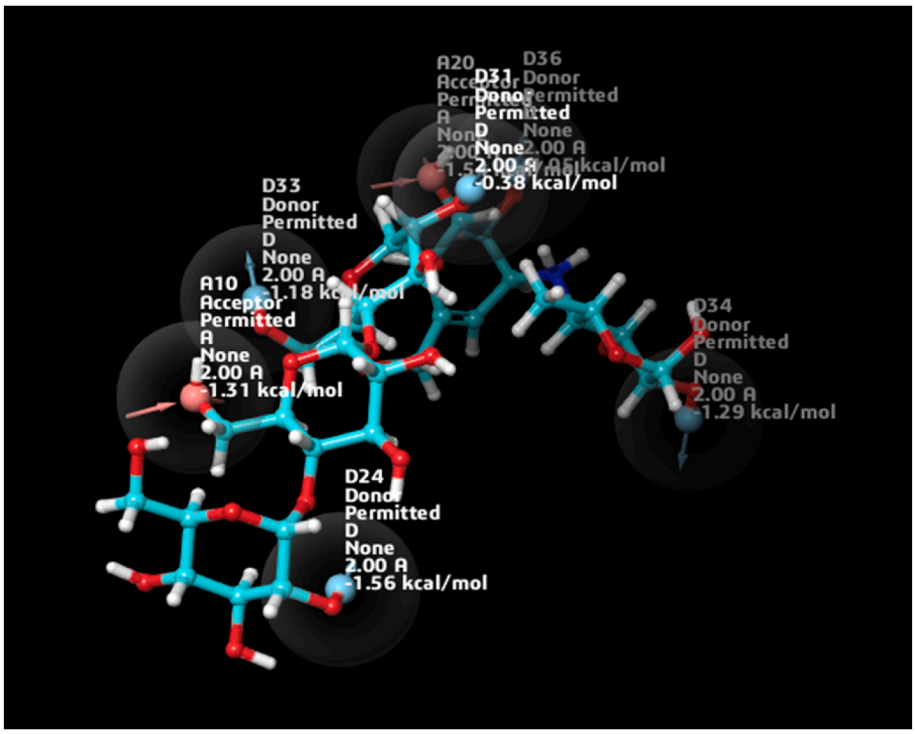

Fig. 5. Pharmacophore hypothesis of α-amylase and acarbose complex.

Table 3
Fitness score of the compounds from pharcophore modeling.

Compound Name	Fitness Scores
Curculin	1.256
Curculigenin A	1.156
Curculigoside	1.133
Acarbose	1.056
Phlorizin	1.003
Curculigenin B	0.984
Pomiferin	0.771
Scandenin	0.297
Stigmasterol	0.09
Sitosterol	0.09
Curculigol	0.002

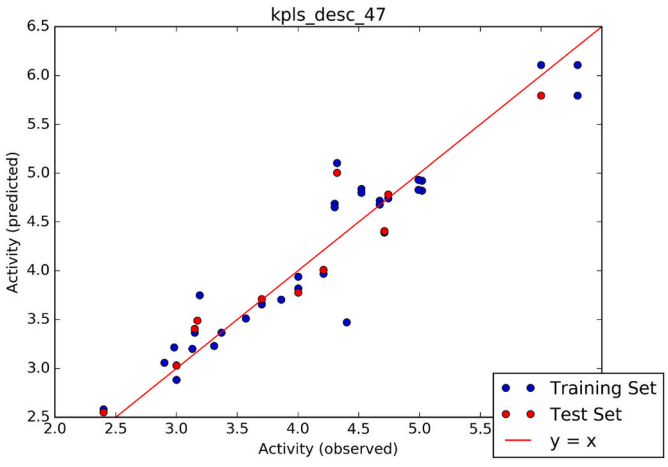

Fig. 6. QSAR scatter plot.

Table 4
pIC50 value of the QSAR modeling of the active compounds.

Compound Name	Pred PIC50 (μM)
Acarbose	6.108
Curculigenin A	5.198
Curculigenin B	5.099
Curculigoside	4.942
Phlorizin	4.929
Pomiferin	4.795
Curculin	4.544
Scandenin	4.507
Stigmasterol	4.328
Sitosterol	4.258
Curculigol	2.321

H-bond observed in the 2D interaction from the post-docking analysis. Curculigoside formed 1.2 intraction fraction with ASP 197 as the heighest H-bond interacting residue. Formation of H-bond between ligand-peotein complex improves binding affinity by introducing hydrogen bond donor and acceptor, establishing strong interaction (Chodera and Mobley, 2013). Based on the findings from this study, curculigoside from *Curculigo pilosa* was predicted as an anti-diabetes compound via α-amylase inhibition. The results from this study agrees with the findings of Ooi et al. (2018) who reported that Curculigoside and polyphenol-rich ethyl acetate fraction of *Molineria latifolia* rhizome improved glucose uptake via potential mTOR/AKT activated GLUT4 translocation. Hence, further study on isolation of this compounds for in vivo experiment and optimization of curculigoside for improved efficacy are suggested.

7. Conclusion

The current study employed in vitro approach to screen three solvent extracts of *C. pilosa* against α-amylase. The bioactive compounds of n-

Table 5
Drug-likeness profile of bioactive compounds.

Compound Name	MW	QPlog^{HERG}	QPP^{Caco}	QPlog^{BB}	QPP^{MDCK}	QPlog^{Khsa}	RO5
Acarbose	645.611	−5.645	0.07	−5.469	0.016	−2.539	3
Curculigenin A	474.723	−4.178	552.44	−1.178	260.491	0.948	0
Curculigenin B	476.738	−4.211	676.30	−1.156	324.153	0.898	0
Curculigoside	466.441	−5.169	37.16	−2.684	14.084	−0.739	1
Curculin	368.385	−6.307	155.01	−2.246	65.952	0.007	0
Phlorizin	436.415	−5.405	9.34	−3.423	3.165	−0.854	1
Pomiferin	420.461	−5.92	337.83	−1.405	153.081	0.974	0
Curculigol	472.793	−4.212	2735.59	−0.417	1468.082	2.041	1
Scandenin	434.488	−5.694	582.57	−1.105	275.877	0.876	0
Sitosterol	414.713	−4.669	3377.57	−0.353	1843.776	2.076	1
Stigmasterol	412.698	−4.526	3377.62	−0.282	1843.811	2.066	1

QPPCaco = Predicted apparent Caco-2 cell permeability in nm/sec; **QPlogBB**= Predicted brain/blood partition coefficient; **RO5**= Rule of five.

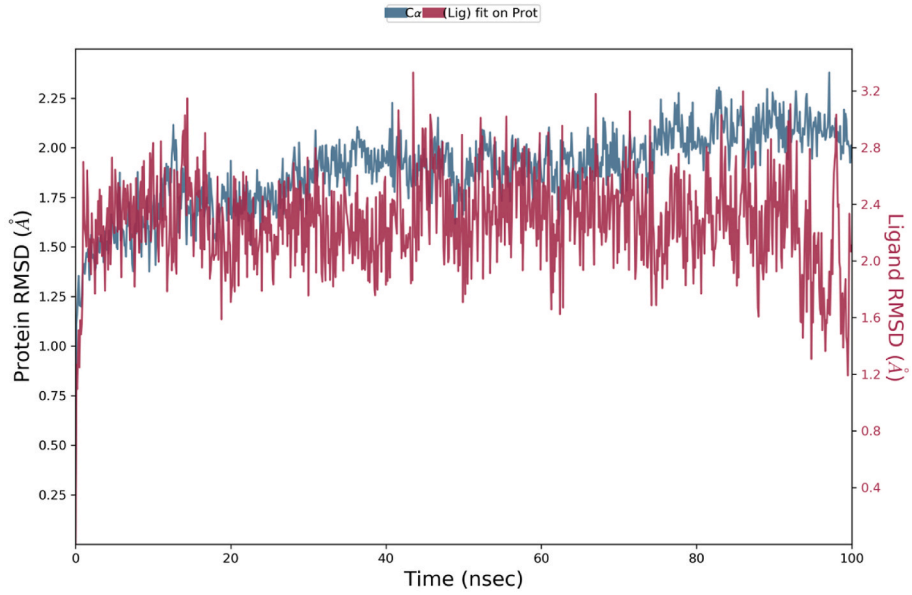

Acarbose

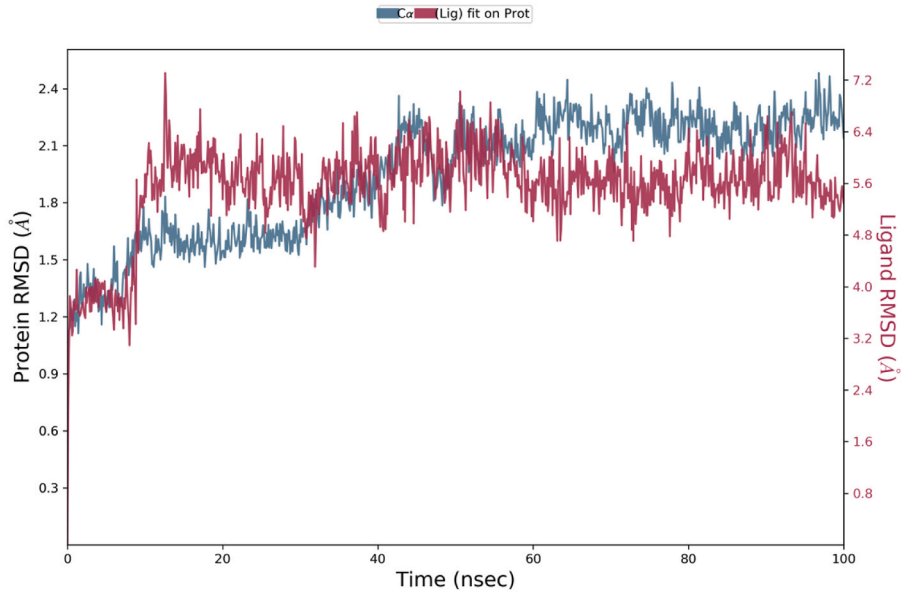

Curculigoside

Fig. 7. Root mean square deviation of ligand-proten complexes.

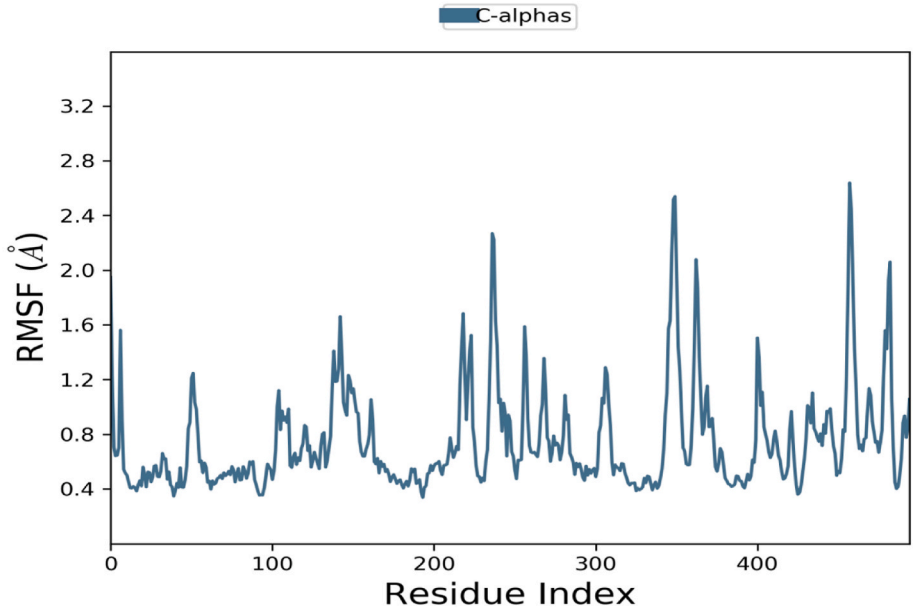

Fig. 8. Root mean square flunctuation of ligand-proten complexes.

butanol, the most active fraction was quantified using HPLC and computational techniques was applied to predict the α-amylase inhibitory potential of these compounds. The plant extracts showed in vitro inhibitory efficacy with n-butanol having the highest percentage inhibition and lowest IC_{50} among the extracts. Of the ten (10) HPLC identified compounds subjected to virtual screening against α-amylase, curculigoside exhibited the heigest binding affinity. All the cpompounds obeyed Lipinski rule of five and within the normal range of pharmacokinetic parameters predicting their drug-likeness property. The MD simulation result of the standard ligand and curculigoside further established their stability within the core of α-amylase for 100 ns simulation period. The data presented from this study can be explore for drug discovery against diabetes.

CRediT authorship contribution statement

Damilola A. Omoboyowa: Writing – original draft, Supervision, Methodology, Funding acquisition, Data curation, Conceptualization. **Temitope C. Aribigbola:** Writing – review & editing. **Simbo T. Akinsulure:** Methodology, Investigation, Data curation. **Damilola S. Bodun:** Writing – review & editing, Resources, Data curation. **Ezekiel A. Olugbogi:** Validation, Software. **Ebenezer A. Oni:** Validation, Software.

Informed consent

Not applicable.

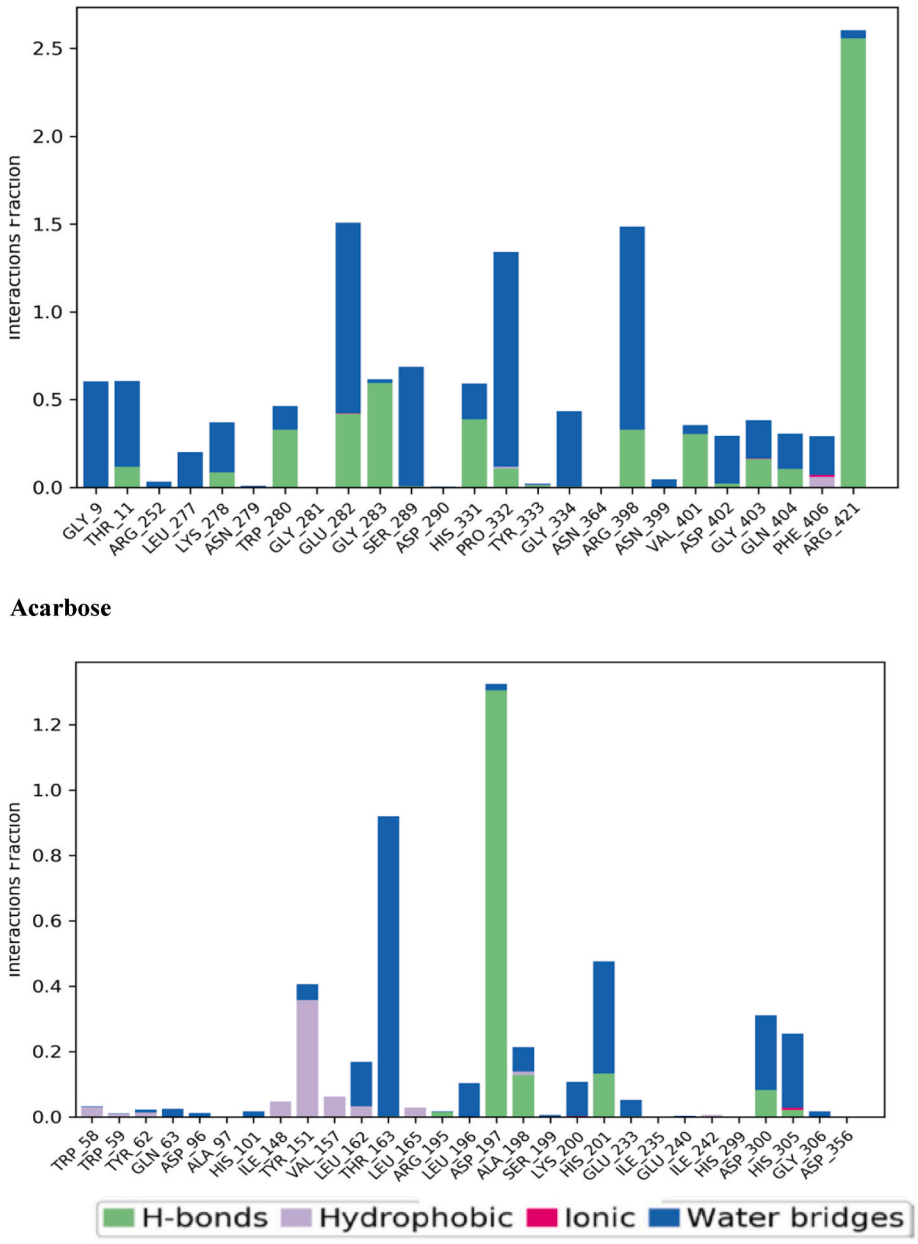

Fig. 9. Bond interaction analysis of ligand-proten complexes.

Ethical approval

Not applicable.

Data availability

Data sharing not applicable to this article as no datasets were generated or analysed during the current study.

Funding

This research was funded by 2024 Adekunle Ajasin University research grant (AAUA_grant_2024).

Declaration of competing interest

The authors declare that they have no known competing financial interests or personal relationships that could have appeared to influence the work reported in this paper.

Appendix A. Supplementary data

Supplementary data to this article can be found online at https://doi.org/10.1016/j.amolm.2025.100064.

References

Aathira, R., Jain, V., 2014. Advances in management of type 1 diabetes mellitus. World J. Diabetes 5, 689. https://doi.org/10.4239/wjd.v5.i5.689.

Adefegha, S.A., Oyeleye, S.I., Oboh, G., 2016. African crocus (*Curculigo pilosa*) and wonderful kola (*Buchholzia coriacea*) seeds modulate critical enzymes relevant to erectile dysfunction and oxidative stress. J. Compl. Integr. Med. https://doi.org/10.1515/jcim-2016-0159.

Balaji, R., Duraisamy, R., Kumar, M.P., 2019. Complications of diabetes mellitus: a review. Drug Invent. Today 12, 98–103.

Barnett, C., Senapathi, T., Bray, S., Goue, N., 2018. Analysis of molecular dynamics simulation. Galaxy Train. Mater. 1, 23–43.
Bhutani, J., Bhutani, S., 2014. Worldwide burden of diabetes. Indian J. Endocrinol. Metabol. 18, 868.
Chike-Ekwughe, A., Adegboyega, A.E., Johnson, T.O., Adebayo, A.H., Ogunlana, O.O., 2023. *In vitro* and in-silico inhibitory validation of *Tapinanthus cordifolius* leaf extract on α-amylase in the management of type 2 diabetes. Inform. Med. Unlocked 36, 101148. https://doi.org/10.1080/07391102.2023.2212791.
Cho, N.H., Shaw, J.E., Karuranga, S., Huang, Y., Da Rocha, J.D., Ohlrogge, A.W., Malanda, B.I.D., 2018. IDF Diabetes Atlas: global estimates of diabetes prevalence for 2017 and projections for 2045. Diabetes Res. Clin. Pract. 138, 271–281. https://doi.org/10.1016/j.diabres.2018.02.023.
Chodera, J.D., Mobley, D.L., 2013. Entropy-enthalpy compensation: role and ramifications in biomolecular ligand recognition and design. Annu. Rev. Biophys. 42, 121–142. https://doi.org/10.1146/annurev-biophys-083012-130318.
Fu, Y., Zhao, J., Chen, Z., 2018. Insights into the molecular mechanisms of protein-ligand interactions by molecular docking and molecular dynamics simulation: a case of oligopeptide binding protein. Comput. Math. Methods Med. 35, 202–214. https://doi.org/10.1155/2018/3502514.
Gbadamosi, I.T., Egunyomi, A., 2010. Phytochemical screening and *in vitro* anti-candidal activity of extracts and essential oil of *Curculigo pilosa* (Schum and Thonn) Engl. Hypoxidaceae. Afr J Biotechnol. 9, 1236–1240. https://doi.org/10.5897/AJB09.1207.
Hollingsworth, S.A., Dror, R.O., 2018. Molecular dynamics simulation for all. Neuron 99, 1129–1143. https://doi.org/10.1016/j.neuron.2018.08.011.
Karigidi, K.O., Ojebode, M.E., Anjorin, O.J., Omiyale, B.O., Olaiya, C.O., 2019. Antioxidant activities of methanol extracts of *Curculigo pilosa* rhizome and *Gladilous psittascinus* corm against lipid peroxidation in rat's liver and heart. J. Herbs, Spices, Med. Plants 25, 1–10. https://doi.org/10.1080/10496475.2018.1510457.
Karigidi, K.O., Olaiya, C.O., 2021. Antidiabetic activity of corn steep liquor extract of Curculigo pilosa and its solvent fractions in streptozotocin-induced diabetic rats. J. Traditional. Complem. Med. 10, 555–564. https://doi.org/10.1016/j.jtcme.2019.06.005.
Kawahito, S., Kitahata, H., 2009. Oshita S. Problems associated with glucose toxicity: role of hyperglycemia-induced oxidative stress. World J. Gastroenterol. 15, 4137. https://doi.org/10.3748/wjg.15.4137.
Kim, S.H., Jo, S.H., Kwon, Y.I., Hwang, J.K., 2011. Effects of onion (*Allium cepa* L.) extract administration on intestinal α-glucosidases activities and spikes in postprandial blood glucose levels in SD rats model. Int. J. Mol. Sci. 12, 3757–3769. https://doi.org/10.3390/ijms12063757.
Korytkowski, M.T., 2004. Sulfonylurea treatment of type 2 diabetes mellitus: focus on glimepiride. Pharmacotherapy. J. Human Pharmacol. Drug Therap. 24, 606–620. https://doi.org/10.1592/phco.24.6.606.34752.
Kwon, S., Bae, V., Jo, J., 2019. Comprehensive ensemble in QSAR prediction for drug discovery. BMC Bioinf. 20, 521. https://doi.org/10.1186/s12859-019-3135-4.
Lipinski, A.C., Lombardo, F., Dominy, B.W., Feeney, P.J., 1997. Experimental and computational approaches to estimate solubility and permeability in drug discovery and development settings. Adv. Drug Deliv. Rev. 23, 3–25. https://doi.org/10.1016/s0169-409x(00)00129-0.
Liu, X., Shi, D., Zhou, S., Liu, H., Liu, H., Yao, X., 2017. Molecular dynamics simulations and novel drug discovery. Expet Opin. Drug Discov. https://doi.org/10.1080/17460441.2018.1403419.
Miller, B.R., Roitberg, A.E., 2013. Design of e-pharmacophore mofels using compound fragments for the trans-sailidase of *Trypanosoma cruzi*: screening for novel inhibitor scaffolds. J. Mol. Graph. Model. 45, 84–97. https://doi.org/10.1016/j.jmgm.2013.08.009.
Nair, S.S., Kavrekar, V., Mishra, A., 2013. In vitro studies on α-amylase and α-glucosidase inhibitory activities of selected plant extracts. Eur. J. Exp. Biol. 3, 128–132.
Natarajan, P., Swargam, S., Hema, K., Vengamma, B., Umamaheswari, A., 2015. E-pharmacophore based virtual screening to identify agonist for PKA-Ca. Biochem. Anal. Biochem. 4, 222–232. https://doi.org/10.4172/2161-1009.1000222.
Nie, Y., Dong, X., He, Y., Yuan, T., Han, T., Rahman, K., 2013. Medicinal plants of genus Curculigo: traditional uses and a phytochemical and ethnopharmacological review. J. Ethnopharmacol. 147, 547–563. https://doi.org/10.1016/j.jep.2013.03.066.
Nursamsiar, N., Nursamsiar, S., Febrina, E., Asnawi, A., Syafie, S., 2022. Synthesis and inhibitory activity of curculigoside A derivatives as potenty anti-diabetes agents with β-cell apoptosis. J. Mol. Struct. 1265, 133292. https://doi.org/10.1016/j.molstruc.2022.133292.
Omoboyowa, D.A., 2022. Exploring molecular docking with E-pharmacophore and QSAR models to predict potent inhibitors of 14-*α*-demethylase protease from *Moringa spp*. Pharmacol. Res. Modern Chinese Med. 4, 100147. https://doi.org/10.1016/j.prmcm.2022.100147.
Omoboyowa, D.A., 2024. Investigation of *Cnidium monnieri* compounds as phosphodiesterase-5 antagonists in erectile dysfunction via molecular docking and dynamic simulation. Inform. Med. Unlocked 45, 101450. https://doi.org/10.1016/j.imu.2024.101450.
Omoboyowa, D.A., Agoi, M.D., Shodehinde, S.A., Saibu, O.A., Saliu, J.A., 2023a. Antidiabetes study of *Spondias mombin* (Linn) stem bark fractions in high-sucrose diet-induced diabetes in *Drosophila melanogaster*. J. Taibah Univ. Med. Sci. 18, 663e675. https://doi.org/10.1016/j.jtumed.2023.01.011.
Omoboyowa, D.A., Aribigbola, T.C., Afolabi, O.F., Joshua, P.E., 2024. *Blighia welwitchii* (Hlem) leaf solvent fractions ameliorate diabetes in *Drosophila melanogaster* induced by high-sucrose diet. Pharmacol. Res. Nat. Prod. 2, 100018. https://doi.org/10.1016/j.prenap.2024.100018.
Omoboyowa, D.A., Bodun, D.S., Saliu, J.A., 2023b. Structure-based *in silico* investigation of antagonists of human ribonucleotide reductase from *Annona muricata*. Inform. Med. Unlocked 38, 101225. https://doi.org/10.1016/j.imu.2023.101225.
Ooi, J., Azmi, N.H., Imam, M.U., Alitheen, N.B., Ismail, M., 2018. Curculigoside and polyphenol-rich ethyl acetate fraction of *Molineria latifolia* rhizome improved glucose uptake via potential mTOR/AKT activated GLUT4 translocation. J. Food Drug Anal. 26 (4), 1253–1264. https://doi.org/10.1016/j.jfda.2018.03.003.
Pace, C.N., Fu, H., Fryar, K.L., Landua, J., Trevino, S.R., Schell, D., Thurlkill, R.L., Imura, S., Scholtz, J.M., Gajiwala, K., Sevcik, J., Urbanikova, L., Myers, J.K., Takano, K., Hebert, E.J., Shirley, B.A., Grimsley, G.R., 2014. Contribution of hydrogen bonds to protein stability. Protein Sci. 23, 652–661. https://doi.org/10.1002/pro.2449.
Tan, S., Lai, A., Cui, R., Bai, R., Li, S., Liang, W., Zhang, G., Jiang, S., Liu, S., Zheng, M., Wang, W., 2019. Curculigoside exerts significant anti-arthritic effects *in vivo* and *in vitro* via regulation of the JAK/STAT/NF-κB signaling pathway. Mol. Med. Rep. 19, 2057–2064. https://doi.org/10.3892/mmr.2019.9854.
Wang, Y., Li, J., Li, N., 2021. Phytochemistry and pharmacological activity of plants of genus Curculigo: an updated review since 2013. Molecules 26, 3396. https://doi.org/10.3390/molecules26113396.
Woolnough, J.W., Monro, J.A., Brennan, C.S., Bird, A.R., 2008. Simulating human carbohydrate digestion in vitro: a review of methods and the need for standardisation. Int. J. Food Sci. Technol. 43, 2245–2256. https://doi.org/10.1111/j.1365-2621.2008.01862.x.
Worthington, V., 1993. α-amylase. Worthington Enzyme Manual. Worthington Biochemical Corporation, New Jersey, United States, pp. 36–41.